

Magnetic frustration in α -NaMnO₂ and CuMnO₂

Ting Jia, Guoren Zhang, Xiaoli Zhang, Ying Guo, Zhi Zeng et al.

Citation: *J. Appl. Phys.* **109**, 07E102 (2011); doi: 10.1063/1.3536533

View online: <http://dx.doi.org/10.1063/1.3536533>

View Table of Contents: <http://jap.aip.org/resource/1/JAPIAU/v109/i7>

Published by the [American Institute of Physics](#).

Related Articles

Thickness effects on the magnetic and electrical transport properties of highly epitaxial LaBaCo₂O_{5.5+δ} thin films on MgO substrates

Appl. Phys. Lett. **101**, 021602 (2012)

Tailoring coercivity of unbiased exchange-coupled ferromagnet/antiferromagnet bilayers

J. Appl. Phys. **112**, 013904 (2012)

Magnetoresistance and magnetocaloric properties involving strong metamagnetic behavior in Fe-doped Ni₄₅(Co_{1-x}Fe_x)₅Mn_{36.6}In_{13.4} alloys

Appl. Phys. Lett. **101**, 012401 (2012)

Mean field renormalization group: A theoretical approach to the Fe_{1-q}Al_q in the bcc lattice

J. Appl. Phys. **111**, 113921 (2012)

Study on spin-splitting phenomena in the band structure of GdN

Appl. Phys. Lett. **100**, 232410 (2012)

Additional information on *J. Appl. Phys.*

Journal Homepage: <http://jap.aip.org/>

Journal Information: http://jap.aip.org/about/about_the_journal

Top downloads: http://jap.aip.org/features/most_downloaded

Information for Authors: <http://jap.aip.org/authors>

ADVERTISEMENT



Special Topic Section:
PHYSICS OF CANCER

Why cancer? Why physics? [View Articles Now](#)

Magnetic frustration in α -NaMnO₂ and CuMnO₂

Ting Jia,¹ Guoren Zhang,¹ Xiaoli Zhang,¹ Ying Guo,¹ Zhi Zeng,^{1,a)} and H. Q. Lin²

¹Key Laboratory of Materials Physics, Institute of Solid State Physics, Chinese Academy of Sciences, Hefei 230031, People's Republic of China

²Department of Physics and Institute of Theoretical Physics, The Chinese University of Hong Kong, Shatin, Hong Kong, People's Republic of China

(Presented 17 November 2010; received 3 September 2010; accepted 26 October 2010; published online 18 March 2011)

The magnetic and electronic properties of α -NaMnO₂ and delafossite CuMnO₂ are investigated using a full-potential linearized augmented plane wave method. For the monoclinic structure at room temperature, CuMnO₂ behaves like a frustrated spin-lattice. For the triclinic structure at low temperature, the obtained magnetic configurations of the lowest energy for both α -NaMnO₂ and CuMnO₂ are consistent with experiments. However, the exchange constants are all positive. This reveals that the magnetic frustration is only partially relieved at low temperature. It is also found that the Mn³⁺ ions are in a high-spin state. Taking into account the on-site Coulomb correlations, our results show that α -NaMnO₂ and CuMnO₂ are charge-transfer insulators. © 2011 American Institute of Physics. [doi:10.1063/1.3536533]

Geometrically frustrated magnetic systems have attracted considerable attention due to their extraordinary magnetic properties.^{1–3} The geometrical frustration is caused by a conflict that arises between the geometry of the space inhabited by a set of degrees of freedom and the local correlations favored by their interactions.^{4,5} The simplest example of a geometrically frustrated system is the triangular-lattice antiferromagnet,^{6–9} in which not all interactions can be minimized simultaneously. With the quasi-two-dimensional (2D) triangular-lattice MnO₂ layers, the compounds AMnO₂ (A = Na, Cu)^{10,11} are of great interest as model compounds for the study of geometrically frustrated magnets. Recently, the crystal structure of α -NaMnO₂ has been reported as the α -NaFeO₂ type,¹⁰ whereas CuMnO₂ is related to the delafossite structure.¹¹ The structure of AMnO₂ is composed of 2D triangular-lattice MnO₂ layers of edge-sharing MnO₆ octahedra separated by A ions, which is monoclinic (*C2/m*) at room temperature (RT) and triclinic (*P1*) at low temperature (LT). But Cu or Na ions are located at the O–Cu–O dumbbell centers or the NaO₆ octahedra centers, respectively. Zorko *et al.*¹² have determined the nearest-neighbor antiferromagnetic (AFM) exchange coupling constants of α -NaMnO₂ at RT by employing the finite-temperature Lanczos method. Stock *et al.*¹³ have described α -NaMnO₂ at LT as a one-dimensional (1D) AFM chain model, in contrast to earlier studies. Zhang *et al.*¹⁴ have performed first-principles density functional calculations for the monoclinic structure of α -NaMnO₂ at RT. However, the electronic structure calculations are absent for α -NaMnO₂ at LT and CuMnO₂ at RT and LT.

Therefore, we intend to perform first-principles calculations to elucidate the electronic structures and magnetic properties of α -NaMnO₂ and CuMnO₂. The magnetic ground state we obtained is in agreement with the experimental findings.^{10,11} And the exchange coupling constants are very similar with the

results of earlier studies.¹³ Importantly, the exchange constants are all positive, which reveals that the magnetic frustration is only partially relieved at LT.

Our calculations were performed by using the standard full-potential linearized augmented plane wave code WIEN2k.¹⁵ The muffin-tin sphere radii were chosen as 2.19, 1.92, and 1.70 a.u. for Na, Mn, and O (α -NaMnO₂) and 1.83, 1.91, and 1.62 a.u. for Cu, Mn, and O (CuMnO₂), respectively. The cutoff parameter $R_{\text{mt}}K_{\text{max}}$ was set to 7.0 and 100 k -points were used over the first Brillouin zone for both α -NaMnO₂ and CuMnO₂. The generalized gradient approximation (GGA) by Perdew *et al.*¹⁶ was employed for the exchange-correlation potential. To properly describe the strong electron correlation associated with the Mn and Cu $3d$ states, we performed GGA + U calculations, where $U_{\text{eff}} = U - J$ (U and J are on-site Coulomb and exchange interaction, respectively) was used instead of U .¹⁷ All the results shown in the following are obtained with $U_{\text{eff}} = 8$ eV, but the use of other U_{eff} values such as 6 and 10 eV leads to qualitatively the same results. To obtain the ground state and the exchange constants, $2 \times 2 \times 2$ supercell calculations were performed for different possible magnetic patterns. Three AFM structures in the Mn–Mn plane [Fig. 1(a)] were I-type (1 \uparrow , 2 \uparrow , 3 \downarrow , 4 \downarrow), II-type (1 \uparrow , 2 \downarrow , 3 \downarrow , 4 \uparrow), and III-type (1 \uparrow , 2 \downarrow , 3 \uparrow , 4 \downarrow) antiferromagnetism. The up arrow (\uparrow) stands for spin-up and the down arrow (\downarrow) stands for spin-down. The prefix *C* denotes ferromagnetic (FM) and *G* denotes AFM interplane couplings. Totally, there are seven possible magnetic configurations for the LT phase [Fig. 1(b)].

The results of GGA and GGA + U calculations for the structure of CuMnO₂ at RT are listed in Table I. Among the five possible magnetic configurations, the I-type antiferromagnetism is the most stable state, which means that AFM exchange is more favorable along the ($\bar{1}10$) and (100) directions. Considering that all the Mn–Mn bonds along the (010) and (100) directions are completely equivalent, both of the (010) and (100) directions should be AFM exchange. Therefore, CuMnO₂ in the

^{a)}Author to whom correspondence should be addressed. Electronic mail: zzeng@theory.issp.ac.cn.

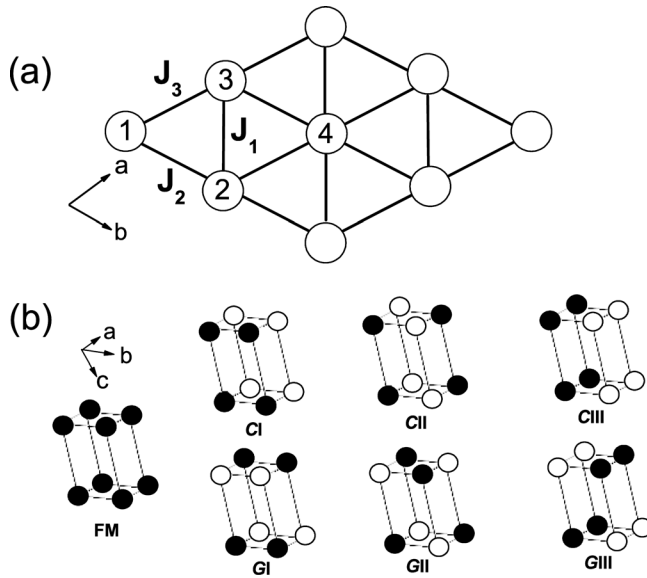


FIG. 1. (a) Magnetic configurations in Mn–Mn plane. (b) Schematic representation of seven magnetic configurations used in our calculations. Only Mn atoms are drawn. Spin-up (\bullet) and spin-down (\circ) moments.

RT structure is a system with frustration effects. In addition, the small difference of total energy between *C* and *G* configurations means that the magnetic coupling between Mn layers is so weak that the system exhibits a 2D characteristic.

The results of GGA and GGA + U calculations for the structure of α -NaMnO₂ (CuMnO₂) in the LT phase are listed in Table II. The 2D characteristic is also obvious. Among the seven magnetic configurations, the CIII (GIII) state is the most stable state for α -NaMnO₂ (CuMnO₂), consistent with experimental observations.^{10,11} In addition, a spin moment of 3.3 (3.4) μ_B /Mn in GGA and 3.7 (3.7) μ_B /Mn in GGA + U is obtained in α -NaMnO₂ (CuMnO₂). The spin-moment corresponds to the high spin state of Mn³⁺ ions ($S=2$). The reduction from the Hund's rule value of 4 μ_B /Mn for $S=2$ is induced by Mn–O hybridization, which is also reflected in the electronic structure discussed in the following.

In order to describe the magnetic frustration and spatially anisotropic exchange interaction more clearly, we estimate the exchange constants along the three triangular directions (three directions are inequivalent in $P\bar{1}$). The nearest-neighbor J_1 , the next-nearest-neighbor J_2 , and the next-next-nearest-neighbor J_3 exchange interactions are taken into account. Since all the configurations (both α -NaMnO₂ and CuMnO₂) exhibit insulating characteristics (see Table II), the spin size of Mn is stable, and the system exhibits a 2D characteristic, a Heisenberg-like Hamiltonian may be a good primary approxi-

TABLE I. The total energy E [meV/(8f. u.)], magnetic moment M (μ_B) per Mn³⁺ and band gap E_g (eV) for the structure of CuMnO₂ at 300 K in different magnetic states.

		Configuration	FM	CI	GI	CII	GII
GGA	E		724	0	5	442	460
	M		3.4	3.3	3.3	3.4	3.4
	E_g		0.1	0.6	0.8	0.6	0.6
GGA + U	E		106	0	3	154	156
	M		3.8	3.8	3.8	3.8	3.78
	E_g		0.9	1.0	1.2	1.0	1.1

mation for the in-plane magnetic energy. By mapping the obtained total energies for each magnetic state to the Heisenberg model, the exchange interactions J_1 , J_2 , and J_3 were calculated within this approximation:

$$2 \times (4 \times 4J_1S^2 + 4 \times 4J_3S^2) = E(FM) - E(CI), \quad (1)$$

$$2 \times (4 \times 4J_2S^2 + 4 \times 4J_3S^2) = E(FM) - E(CII), \quad (2)$$

$$2 \times (4 \times 4J_1S^2 + 4 \times 4J_2S^2) = E(FM) - E(CIII), \quad (3)$$

as the values of the exchange constants from GGA calculations are more reliable,¹⁴ we adopt the GGA results. With the moment $S=2$, we get $J_1=5.7$ meV, $J_2=2.3$ meV, and $J_3=2.1$ meV for α -NaMnO₂ and $J_1=4.8$ meV, $J_2=1.3$ meV, and $J_3=0.9$ meV for CuMnO₂. The value of J_1 for α -NaMnO₂ is very similar with the one obtained by Stock *et al.*¹³ and also does not change drastically after the structural phase transition, since the value of J_1 for α -NaMnO₂ in the LT phase is nearly the same as the one obtained in the RM phase.^{12,14} In addition, The value of J_1 is much larger than that of J_2 and J_3 . So the intrachain interactions (J_1) are dominate in these compounds.

Importantly, all the values of J_1 , J_2 , and J_3 being positive means that the AFM interaction is the minimum energy state for the three directions, although FM ordering is formed along J_3 . Such AFM interaction originates from the Mn–Mn direct exchange interactions. As we know, all the Mn–O–Mn super-exchange interactions are weak due to the nearly 90° angles.¹⁸ So Mn–Mn direct exchange interactions in-plane should be dominant. And half-filled t_{2g} orbitals directed along the three triangular directions should favor strong AFM direct exchange between Mn³⁺ ions.¹⁸ Since all AFM interactions cannot be satisfied simultaneously, the interaction of relative longer Mn-Mn distance (J_3) is forced to FM coupling under competition. Therefore, despite the onset of the long-range magnetic order, α -NaMnO₂ and CuMnO₂ can still be regarded as a frustrated system.

TABLE II. The total energy E [meV/(8f. u.)], magnetic moment M (μ_B) per Mn³⁺ and band gap E_g (eV) for the structure of α -NaMnO₂ (CuMnO₂) at 4 K (10 K) in different magnetic states.

		Configuration	FM	CI	GI	CII	GII	CIII	GIII
GGA	E		1018(755)	15(29)	15(33)	500(464)	496(481)	0(0)	1(6)
	M		3.4(3.4)	3.3(3.3)	3.3(3.3)	3.3(3.4)	3.3(3.4)	3.3(3.3)	3.3(3.3)
	E_g		0.9(0.1)	1.3(0.6)	1.3(0.8)	1.2(0.6)	1.3(0.6)	1.4(0.6)	1.3(0.8)
GGA + U	E		204(132)	5(12)	6(10)	145(160)	143(166)	0(1.2)	1(0)
	M		3.7(3.7)	3.7(3.7)	3.7(3.7)	3.7(3.7)	3.7(3.7)	3.7(3.7)	3.7(3.7)
	E_g		2.3(1.2)	2.9(1.3)	2.8(1.5)	2.9(1.3)	2.9(1.4)	2.9(1.3)	2.8(1.4)

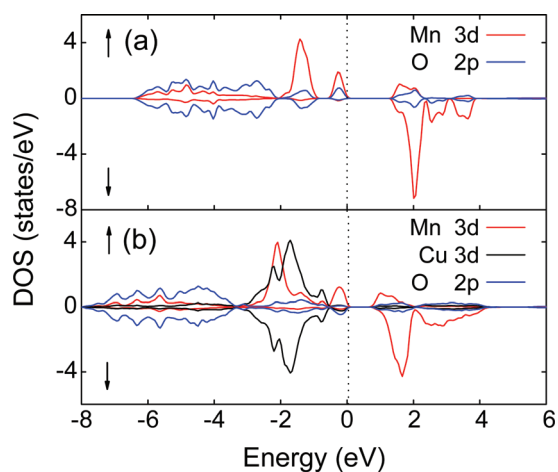


FIG. 2. (Color online) Partial density of states (DOS) of (a) α -NaMnO₂ [(b) CuMnO₂] by GGA in the CIII (GIII) state for the fixed structure at 4 K (10 K). The 2p states are of two oxygens in one formula unit.

The partial density of states (DOS) of GGA calculations for the structure of α -NaMnO₂ and CuMnO₂ in the LT phase are presented in Fig. 2. As shown in Fig. 2(a), α -NaMnO₂ is insulating with a band gap of 1.4 eV. In the approximately octahedral crystal field, the d manifold splits into lower t_{2g} and upper e_g states. And the e_g orbitals are further split into $d_{3z^2-r^2}$ and $d_{x^2-y^2}$ due to the JT distortion that all octahedra are axially elongated along the same direction. The corresponding t_{2g} and e_g manifolds of the Mn 3d states can be easily distinguished in Fig. 2(a): states derived by $t_{2g\uparrow}$ and lowered $d_{3z^2-r^2\uparrow}$ are located between -2 and -1 eV, -0.8 and 0 eV, the Mn $d_{x^2-y^2\uparrow}$ and d_{\downarrow} states are nearly empty and are placed at approximately 2 eV above the Fermi level. Thus, the Mn ions are in the high-spin state. The O 2p band is below the Mn 3d bands and lies about 4 eV below the Fermi level with a bandwidth of approximately 4 eV. In addition, the O 2p states also experience a substantial polarization in the same energy area as the $d_{3z^2-r^2\uparrow}$ band, due to the strong σ -type overlap with e_g states. A similar DOS of GIII-ordered CuMnO₂ are shown in Fig. 2(b). The fulfilled Cu 3d states are located between -3 and -0.5 eV. Therefore, Cu occurs as Cu¹⁺ in this material.

Although α -NaMnO₂ and CuMnO₂ are already insulating within GGA, the strong correlation between d electrons of Mn and Cu ions should not be neglected. Therefore, on-site Coulomb correlations of the Mn and Cu 3d electrons are taken into account by using a GGA + U method with $U_{\text{eff}} = 8$ eV. Compared with GGA results, the Cu bands are little shifted due to the closed shell configuration of the Cu⁺ ion, whereas the occupied Mn 3d bands are shifted downward both in α -NaMnO₂ and CuMnO₂ (Fig. 3). The DOS has a large contribution from the O 2p states and a small contribution from the Mn 3d states in the occupied regions from -4 (-6) to 0 eV in α -NaMnO₂ (CuMnO₂). This is due to the strong electron–electron repulsion, which pushes the occupied bands down. Because of this shift, the character of the increased band gap is predominantly a charge-transfer gap from the O 2p to Mn 3d orbitals.

In summary, we have studied the magnetic properties and electronic structure of α -NaMnO₂ and delafossite CuMnO₂

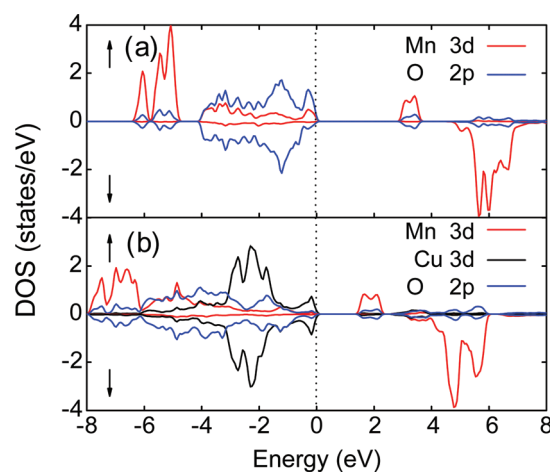


FIG. 3. (Color online) Partial density of states (DOS) of (a) α -NaMnO₂ [(b) CuMnO₂] by GGA + U ($U_{\text{eff}} = 8$ eV) in the CIII (GIII) state for the fixed structure at 4 K (10 K). The 2p states are of two oxygens in one formula unit.

using GGA and GGA + U approaches. Like α -NaMnO₂, the triangular-lattice of CuMnO₂ exhibits magnetic frustration at RT. And at LT, accompanied by a structural phase transitions from monoclinic ($C2/m$) to triclinic ($P\bar{1}$), a long-range ordered AFM ground state is formed in both α -NaMnO₂ and CuMnO₂. However, the magnetic frustration is only partially relieved: despite the onset of the long-range magnetic order, the AFM interaction is the minimum energy state for all three directions. Thus, α -NaMnO₂ and CuMnO₂ can still be regarded as frustrated systems. The GGA calculations describe a high-spin state of Mn³⁺ ions: The JT distortion lowers the energy of $d_{3z^2-r^2}$ orbital, leading to the stabilization of high-spin Mn. Our GGA + U results show that α -NaMnO₂ and CuMnO₂ are charge-transfer insulators.

We thank C. Stock for providing the structural parameters. The author gratefully acknowledges the support of K.C. Wong Education Foundation, Hong Kong. This work was supported by the special Funds for Major State Basic Research Project of China (973) under Grant No. 2007CB925004, Knowledge Innovation Program of Chinese Academy of Sciences under Grant No. KJCX2-YW-W07, and Director Grants of CASHIPS, CUHK Direct Grant No. 2060345. Part of the calculations were performed in the Center for Computational Science of CASHIPS and the Shanghai Supercomputer Center.

- ¹T. Kimura *et al.*, *Nature (London)* **426**, 55 (2003).
- ²N. Hur *et al.*, *Nature (London)* **429**, 392 (2004).
- ³T. Lottermoser *et al.*, *Nature (London)* **430**, 541 (2004).
- ⁴J. E. Greedan, *J. Mater. Chem.* **11**, 37 (2001).
- ⁵R. Moessner and A. P. Ramirez, *Phys. Today* **59**, 24 (2006).
- ⁶A. J. W. Reitsma *et al.*, *New J. Phys.* **7**, 121 (2005).
- ⁷F. Ye *et al.*, *Phys. Rev. Lett.* **99**, 157201 (2007).
- ⁸D. J. Singh, *Phys. Rev. B* **55**, 309 (1997).
- ⁹T. Jia *et al.*, *Phys. Rev. B* **80**, 045103 (2009).
- ¹⁰M. Giot *et al.*, *Phys. Rev. Lett.* **99**, 247211 (2007).
- ¹¹F. Damay *et al.*, *Phys. Rev. B* **80**, 094410 (2009).
- ¹²A. Zorko *et al.*, *Phys. Rev. B* **77**, 024412 (2008).
- ¹³C. Stock *et al.*, *Phys. Rev. Lett.* **103**, 077202 (2009).
- ¹⁴G. R. Zhang *et al.*, *J. Appl. Phys.* **105**, 07E512 (2009).
- ¹⁵P. Blaha *et al.*, see <http://www.wien2k.at>.
- ¹⁶J. P. Perdew *et al.*, *Phys. Rev. Lett.* **77**, 3865 (1996).
- ¹⁷S. L. Dudarev *et al.*, *Phys. Rev. B* **57**, 1505 (1998).
- ¹⁸J. B. Goodenough, *Phys. Rev.* **117**, 1442 (1960).